Current Biology, Vol. 13, 1378–1387, August 19, 2003, ©2003 Elsevier Science Ltd. All rights reserved. DOI 10.1016/S0960-9822(03)00538-4

Arabidopsis Sterol Endocytosis Involves Actin-Mediated Trafficking via ARA6-Positive Early Endosomes

Markus Grebe,[1,5,*] Jian Xu,[1] Wiebke Möbius,[2] Takashi Ueda,[3] Akihiko Nakano,[3] Hans J. Geuze,[2] Martin B. Rook,[4] and Ben Scheres[1,*]

[1]Department of Molecular Cell Biology
Utrecht University
Padualaan 8
3584 CH Utrecht

[2]Department of Cell Biology
University Medical Centre Utrecht
Heidelberglaan 100
3584 CX Utrecht
The Netherlands

[3]Molecular Membrane Biology Laboratory
RIKEN
2-1 Hirosawa
Wako
Saitama 351-0198
Japan

[4]Department of Medical Physiology
University Medical Centre
Universiteitsweg 100
3584 CG Utrecht
The Netherlands

Summary

Background: In contrast to the intense attention devoted to research on intracellular sterol trafficking in animal cells, knowledge about sterol transport in plant cells remains limited, and virtually nothing is known about plant endocytic sterol trafficking. Similar to animals, biosynthetic sterol transport occurs from the endoplasmic reticulum (ER) via the Golgi apparatus to the plasma membrane. The vesicle trafficking inhibitor brefeldin A (BFA) has been suggested to disrupt biosynthetic sterol transport at the Golgi level.

Results: Here, we report on early endocytic sterol trafficking in *Arabidopsis* root epidermal cells by introducing filipin as a tool for fluorescent sterol detection. Sterols can be internalized from the plasma membrane and localize to endosomes positive for the early endosomal Rab5 GTPase homolog ARA6 fused to green fluorescent protein (GFP) (ARA6-GFP). Early endocytic sterol transport is actin dependent and highly BFA sensitive. BFA causes coaccumulation of sterols, endocytic markers like ARA6-GFP, and PIN2, a polarly localized presumptive auxin transport protein, in early endosome agglomerations that can be distinguished from ER and Golgi. Sterol accumulation in such aggregates is enhanced in *actin2* mutants, and the actin-depolymerizing drug cytochalasin D inhibits sterol redistribution from endosome aggregations.

Conclusions: Early endocytic sterol trafficking involves transport via ARA6-positive early endosomes that, in contrast to animal cells, is actin dependent. Our results reveal sterol-enriched early endosomes as targets for BFA interference in plants. Early endocytic sterol trafficking and recycling of polar PIN2 protein share a common pathway, suggesting a connection between plant endocytic sterol transport and polar sorting events.

*Correspondence: markus.grebe@genfys.slu.se (M.G.), b.scheres@bio.uu.nl (B.S.)

[5]Present address: Umeå Plant Science Centre, Department of Forest Genetics and Plant Physiology, Swedish University of Agricultural Sciences, SE-901 83 Umeå, Sweden.

Introduction

Sterols comprise lipid components of eukaryotic membranes that determine membrane characteristics and are required for polar sorting events during vesicle transport in animal cells [1]. Cholesterol-dependent vesicle transport contributes to the establishment of cell polarity in *Caenorhabditis* [2] and pattern formation during *Drosophila* wing development [3]. Several human genetic disorders are caused by defects in cholesterol trafficking in the late endocytic/lysosomal pathway [4].

Endocytic organelles of animal cells have been defined based on the flow of cargo molecules that, upon internalization, are transported to early endosomes. From there, they can be distributed to late endosomes and to lysosomes. Alternatively, molecules may be recycled directly from early endosomes to the plasma membrane (PM) or indirectly via recycling endosome compartments [5]. Next to its predominant PM localization, cholesterol is highly abundant at the *trans*-Golgi [6], enriched in recycling endosomes [7–9], and, to a low extent, detectable in early and late endosomes as well as lysosomes [8, 9]. Both membrane trafficking and fusion throughout the endocytic pathway are regulated by small Rab-type GTPases [10]. Rab5 colocalizes with cholesterol and regulates its distribution in early endosomes [8]. Moreover, Rab5 mediates early endosome movement along microtubules [11]. In general, the integrity of animal endosomal compartments depends on an intact microtubule cytoskeleton [12]. Similarly, biosynthetic cholesterol trafficking from the endoplasmic reticulum (ER) via the Golgi toward the PM is tubulin dependent [13]. Along the biosynthetic route, the vesicle trafficking inhibitor brefeldin A (BFA) disrupts cholesterol trafficking at the Golgi [13, 14].

In comparison to animal cells, plant endocytosis remains ill defined [15, 16]. Some recent studies report the internalization of plant PM proteins and cell wall pectins [17–19]. The *Arabidopsis* PIN1 and PIN2 proteins represent polarly localized presumptive transporters for the plant hormone auxin, and PIN1 recycles between the PM and a BFA-induced endomembrane compartment [17, 20]. Several markers for the endocytic pathway in plants have been established only recently. These include styryl dyes like FM4-64, commonly used to study endocytosis in yeast and animal cells, and the *Arabidopsis* Rab5 homologs ARA6 and ARA7 [18, 21]. Consistent with localization to early endosomes, green fluorescent protein (GFP) fusions to ARA6 and ARA7 colocalize with FM4-64 early upon its internalization into protoplasts [21].

Despite critical roles for cholesterol endocytosis in animals, knowledge about plant sterol trafficking remains restricted to biosynthetic transport. Plant sterol biosynthesis has been extensively characterized by biochemical approaches [22] that also revealed biosynthetic transport from the ER via the Golgi toward the PM, where sterols accumulate at steady state [23]. BFA is generally considered to act as an inhibitor of secretion in plants [24] and has been suggested to interfere with biosynthetic sterol trafficking at the Golgi in leek seedlings [23].

Here, we analyze endocytic sterol trafficking in the *Arabidopsis* root epidermis, a system for studying vesicular transport in a multicellular context. Early endocytic sterol trafficking involves transport via ARA6-positive early endosomes and reveals sterol-enriched endosomes as BFA targets in plants. In contrast to animal cells, endocytic sterol transport via early endosomes is actin dependent.

Results

Subcellular Sterol Distribution

In animal cells, the sterol binding antibiotic filipin is routinely used for fluorescent and ultrastructural detection of free cholesterol [1, 6–8, 14]. By modifying protocols for cholesterol localization, we established filipin as a probe for fluorescent detection of plant 3-β-hydroxysterols. Filipin specifically detected 3-β-hydroxysterols on blots and in *Arabidopsis* roots (see Figure S1 in the Supplemental Data available with this article online). Subsequently, we analyzed sterol distributions in epidermal cells by colocalizing filipin-sterol fluorescence with green or yellow fluorescent proteins (GFP or YFP) targeted to different organelles [25–29]. As a PM marker, we employed enhanced GFP (EGFP) fused to the low-temperature-inducible protein LTI6a (also called rapidly cold-inducible 2a, RCI2a) [28], a member of a family of conserved, small, integral PM proteins [30, 31]. *Arabidopsis LTI6a/RCI2a* encodes a functional homolog of yeast Pmp3p originally purified as a PM proteolipid [31]. Filipin-sterol fluorescence was predominantly observed at the cell periphery (Figures 1C–1F), where it colabeled with EGFP-LTI6a (Figures 1C and 2). At the ultrastructural level, filipin-sterol complexes formed characteristic 20–30 nm protruberances at the PM (Figure 1B). Filipin-sterol fluorescence also accumulated in intracellular compartments (Figures 1C–1E). We observed little overlap between sterols and the distribution of ER-targeted proteins such as mGFP5-ER and EGFP-Q4 (Figure 1G; data not shown for EGFP-Q4). Similarly, little colabeling of sterols was found with Golgi-targeted *N*-acetylglucosaminyl transferase I [29] fused to EGFP (NAG-EGFP) (Figure 1F). As a second Golgi marker, we utilized rat *N*-α-2,6-sialyltransferase fused to YFP (*N*-ST-YFP). In *Arabidopsis* roots, rat α-2,6-sialyltransferase localizes to cisternae and membranes of the *trans* side of the Golgi [32], and a fluorescent protein fusion localizes to the *trans* side of Golgi stacks in tobacco [26]. Sterols partially colabeled with *N*-ST-YFP (Figure 1E). Similarly, we observed partial overlap of filipin-sterol fluorescence and the early endosomal Rab5 homolog ARA6 fused to GFP (Figure 1D). Consistently, ARA6-GFP and GFP fusions of two other Rab5 homologs (ARA7 and RHA1) partially colabeled with filipin-sterol fluorescence in protoplasts (data not shown), and this colocalization pattern is reminiscent of filipin-cholesterol colocalization with Rab5-GFP in animal cells [8]. Our results demonstrate that *Arabidopsis* sterols are abundant in the PM and may also localize to the *trans*-Golgi. Furthermore, they reveal ARA6-positive early endosomes as novel sterol-enriched compartments in plants.

In Vivo Sterol Internalization

To analyze sterol internalization, we pulse labeled live *Arabidopsis* roots expressing EGFP-LTI6a with filipin and examined epidermal cells for filipin-sterol fluorescence. Subsequent to filipin labeling and wash out, filipin-sterol fluorescence occurred at the PM (Figure 2). After 30 min of incubation in filipin-free medium, sterol fluorescence appeared in internal compartments, while steady-state EGFP-LTI6a localization remained unaffected (Figure 2). These findings suggest that sterols are internalized in the *Arabidopsis* root epidermis and support that endocytic sterol trafficking occurs in plant cells.

BFA-Sensitive Early Endocytic Sterol Trafficking

We next analyzed BFA effects on sterol trafficking in the *Arabidopsis* root epidermis. In epidermal cells, 25 μM BFA caused strong coaccumulation of sterols and EGFP-LTI6a in discrete subcellular compartments as early as 5–30 min after application (Figures 3A–3C). Similarly, EGFP-LTI6a rapidly colabeled with the endocytosis marker FM4-64 in BFA-induced compartments (Figures 3D and 3E). These results suggest that sterol-enriched BFA compartments contain early endosomes. Consistent with this view, ARA6-GFP partially colabeled with sterols in BFA-induced structures (Figure 3F). Under the same conditions, sterol-containing compartments did not accumulate ER-targeted proteins (Figure 3G). Notably, early BFA-induced sterol compartments could be distinguished from the Golgi. Both Golgi markers *N*-ST-YFP (Figure 3H) and NAG-EGFP (Figure 3I) mainly localized to multiple discrete, punctate structures that surrounded sterol-containing compartments and likely represented individual Golgi stacks. A low degree of colabeling between *N*-ST-YFP and sterols, however, was observed in sterol-containing structures (Figure 3H, inset) and suggests that some *trans*-Golgi material may contribute to sterol-containing BFA compartments. Consistent with these results, ultrastructural analyses revealed that BFA-induced agglomeration of a mixed vesicle population that contained only some *trans*-Golgi-derived material was devoid of ER and was surrounded by Golgi stacks (Figures 4A–4C). Together, our findings suggest that BFA induces agglomeration of sterol-containing vesicles that partially represent early endosomes.

We further examined whether components in BFA compartments derive from the PM by double pulse labeling plants that expressed EGFP-LTI6a with filipin and FM4-64. All three components colabeled in the center of BFA compartments (Figure 3K), demonstrating that

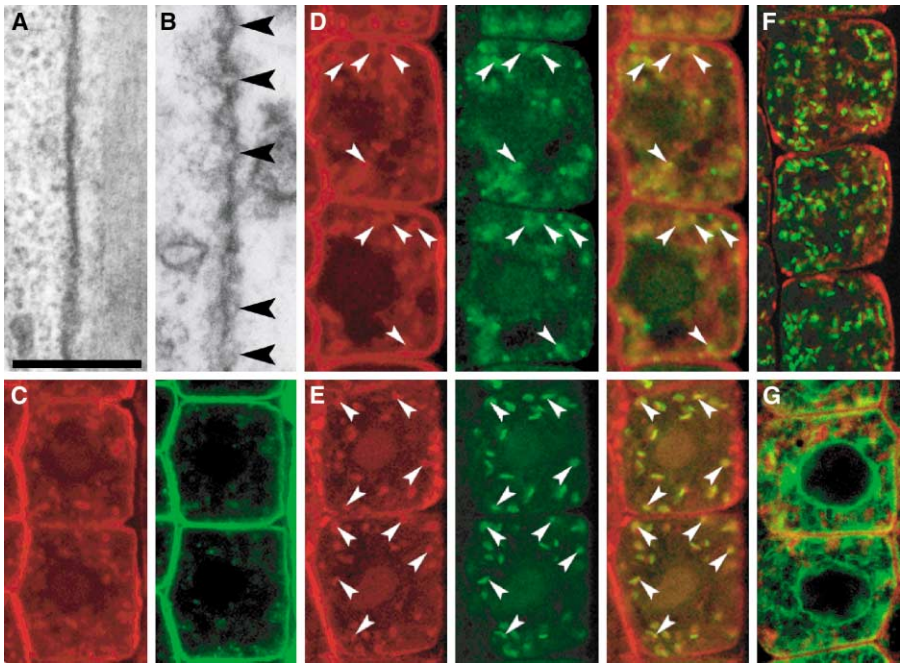

Figure 1. Subcellular Localization of 3-β-Hydroxysterols in *Arabidopsis* Root Epidermal Cells

(A and B) Ultrastructural detection of filipin-sterol complexes at the PM. (A) Untreated. (B) Filipin treated. Note the protuberances of the filipin-sterol complexes (arrowheads). The scale bar represents 200 nm.

(C–G) Double staining for filipin-sterol fluorescence (red) and fluorescent proteins (green) targeted to different membrane compartments. Fluorescence images are in false colors and show aldehyde-fixed cells. Double labeling with (C) EGFP-LTI6a, (D) ARA6-GFP, (E) *N*-ST-YFP, (F) NAG-EGFP, and (G) mGFP5-ER. (D and E) The arrowheads indicate colabeling structures. The right panels represent merged channels.

sterol- and FM4-64-positive material in these structures derives from the PM. To establish the fate of PM proteins accumulating in BFA compartments, we analyzed trafficking of newly synthesized EGFP-LTI6a under BFA treatment by fluorescent recovery after photobleaching (FRAP). After bleaching of EGFP-LTI6a fluorescence, de novo synthesized protein rapidly reappeared at the PM, while recovery in BFA compartments occurred with an approximate 30-min delay (30 ± 5 min, n = 5 roots) (Figures 3L and 3M). By contrast, BFA did not significantly influence FRAP of EGFP-LTI6a at the PM, when compared to samples that were not treated with the inhibitor (Figure S2B in the Supplemental Data). Thus, BFA does not primarily affect EGFP-LTI6a targeting to the PM, but rather a later trafficking step likely to involve endocytosis.

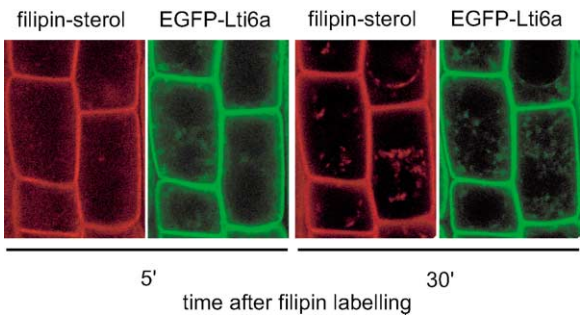

Figure 2. Filipin-Sterol Internalization in Live Epidermal Cells

Arabidopsis roots expressing EGFP-LTI6a (green) pulse labeled with filipin (red) 5 and 30 min after labeling.

We addressed whether EGFP-LTI6a in BFA compartments derived from the PM rather than from a biosynthetic pathway. Application of cycloheximide (CHX) did not obviously influence steady-state levels of EGFP-LTI6a at the PM (Figures 3N and 3O), but it effectively inhibited FRAP of EGFP-LTI6a (Figure S2C in the Supplemental Data). These findings suggest that biosynthesis does not strongly contribute to the PM pool of this protein at steady state, and they indicate that it is not rapidly degraded. CHX preincubation and the subsequent addition of BFA did not obviously influence accumulation of EGFP-LTI6a in BFA compartments (Figures 3P and 3Q). Thus, similar to PIN1 in vascular cells [17], accumulation of EGFP-LTI6a in epidermal BFA compartments occurred largely independent of protein biosynthesis. Since PM-derived sterols and EGFP-LTI6a rapidly colocalized with early endosomal markers upon BFA treatment, our data strongly suggest that BFA interferes with early endocytic sterol trafficking.

Actin-Dependent Early Endocytic Sterol Trafficking

To elucidate cytoskeletal requirements of endocytic sterol trafficking, we examined the effects of actin and tubulin inhibitors on subcellular sterol distributions. Application of the tubulin-depolymerizing drugs oryzalin or nocodazole did not affect subcellular sterol distributions in elongating cells (data not shown). By contrast, appli-

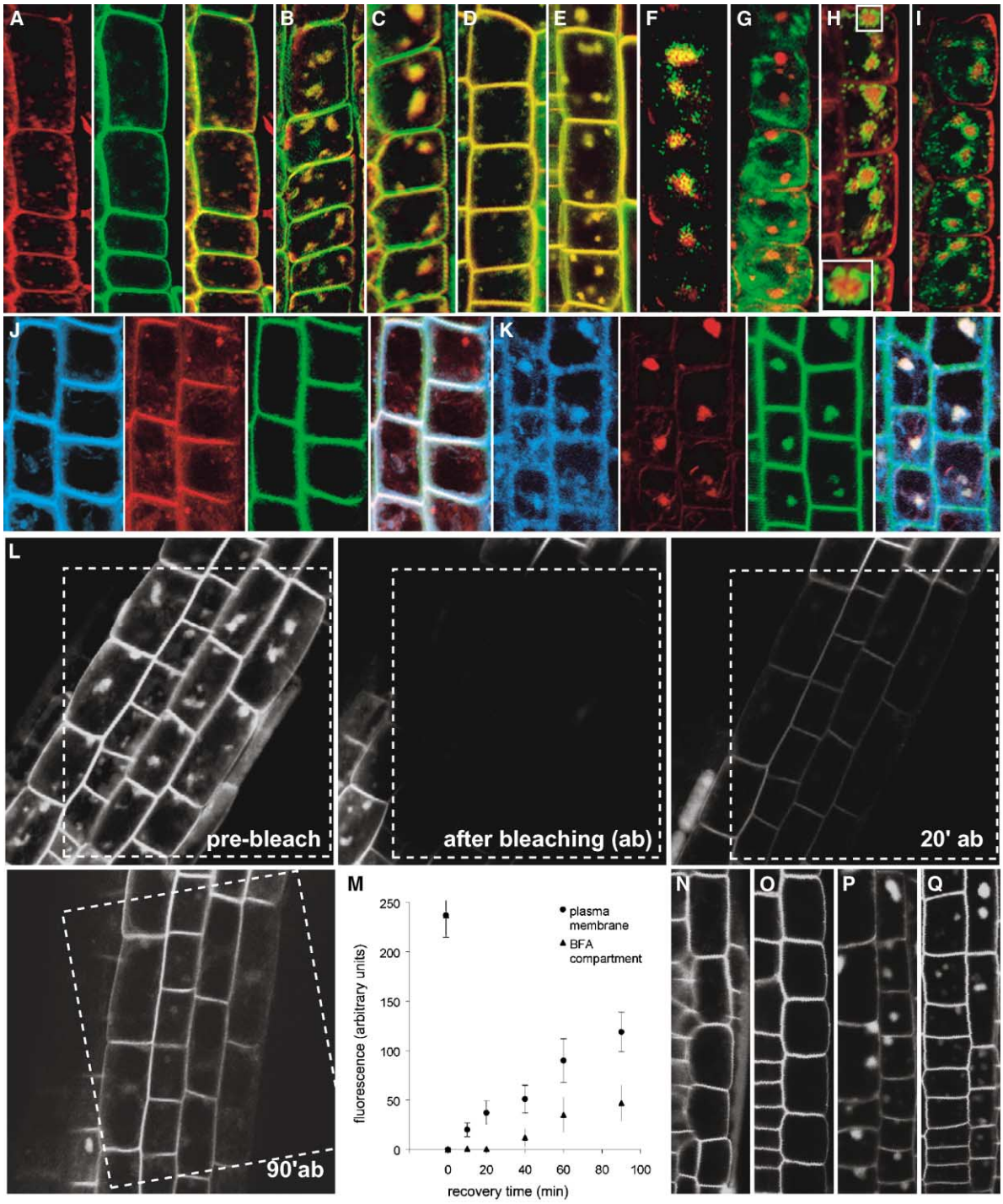

Figure 3. BFA-Induced Sterol Accumulation in Early Endosomal Aggregates

(A–C) Filipin-sterol (red) and EGFP-LTI6a (green) fluorescence in epidermal cells treated with BFA and fixed in aldehyde. (A) A 5-min incubation with 25 μM BFA. Right, merged channels. (B) Merged channels at 15 min of incubation with 25 μM BFA. (C) Merged channels at 30 min of incubation with 25 μM BFA.

(D and E) FM4-64 (red) internalization and EGFP-LTI6a (green) fluorescence in live epidermal cells after (D) 5 min of incubation with 25 μM BFA and (E) 30 min of incubation with 25 μM BFA.

(F–I) Filipin-sterol (red) and GFP/YFP fluorescence (green) in epidermal cells fixed after 30 min of incubation with 25 μM BFA. Filipin-sterol and (F) ARA6-GFP, (G) mGFP5-ER, (H) *N*-ST-YFP, and (I) NAG-EGFP. The inset in (H) shows higher magnification of a BFA compartment.

(J and K) Filipin-sterol (blue), FM4-64 (red), and EGFP-LTI6a (green) fluorescence in live epidermal cells after filipin and FM4-64 pulse labeling, followed by 1 hr of incubation (J) without or (K) with 100 μM BFA. The right panels in (J) and (K) are merged channels.

(L and M) FRAP analysis of EGFP-LTI6a bleached after 1 hr of incubation with 50 μM BFA pretreatment and observed for FRAP under continuous incubation in 50 μM BFA at the indicated time points. (L) The frames indicate areas of photobleaching. (M) Extended quantitative analyses of the experiment in (L). The error bars indicate standard deviations from the average of measurements from four cells (see the Supplemental Data).

(N–Q) EGFP-LTI6a fluorescence in live roots. (N) Untreated. (O) 2.5 hr of incubation with 50 μM CHX. (P) 2 hr of incubation with 50 μM BFA. (Q) Preincubation for 30 min with 50 μM CHX, followed by a 2-hr incubation with 50 μM BFA, 50 μM CHX.

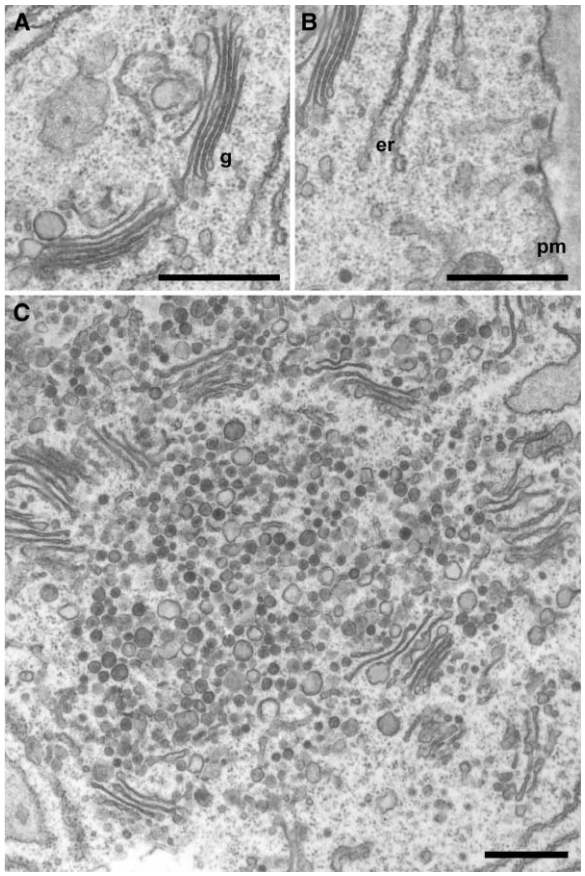

Figure 4. Ultrastructure of a BFA Compartment in an Elongating Epidermal Cell

(A and B) Without BFA treatment. Golgi (g), ER (er), and PM (pm). (C) BFA compartment after 30 min of incubation with 25 μM BFA. The scale bars represent 500 nm.

cation of the actin-depolymerizing drug cytochalasin D (cytD) caused sterol accumulation in small intracellular compartments (Figure 5A). These differed by their higher number and smaller size from BFA-induced endosome agglomerations but, similarly, coaccumulated sterols and EGFP-LTI6a (Figure 5A). FRAP analysis of roots pretreated with cytD revealed fluorescence recovery of EGFP-LTI6a at the PM, while hardly any recovery was observed in intracellular compartments (Figure 5E). These results indicate a strong cytD effect on the endocytic pathway of the sterol colocalizing PM protein. Together, our results suggest that early endocytic sterol and EGFP-LTI6a trafficking require the actin cytoskeleton.

We further examined whether interference with the actin cytoskeleton affects trafficking of sterol-containing early endosomes. Application of cytD caused coaccumulation of sterols and ARA6-GFP (Figure 5B) as well as colocalization of FM4-64 and ARA6-GFP (data not shown) in cytD-induced compartments. These findings suggest that sterol-enriched cytD compartments contain early endosomes. Additionally, some sterol- or FM4-64-containing cytD compartments coaccumulated Golgi markers (Figures 5C and 5D; data not shown for FM4-64), indicating that cytD treatment causes agglomeration or partial fusion of early endosomes and the Golgi. These results suggest that, similar to transport of Golgi stacks [26], trafficking of sterol-enriched early endosomes requires the actin cytoskeleton.

Actin-Dependent Sterol Redistribution from Endosomes

We investigated whether sterols can redistribute from endosomal aggregates. To this end, we examined the reversibility of sterol accumulation after inhibitor treatment and found that the effects of even prolonged incubation with either cytD or BFA were reversible after drug wash out (Figures 6A–6E). Application of cytD after BFA treatment and wash out inhibited sterol redistribution from BFA compartments (Figure 6F), and this inhibition suggests that sterol redistribution from endosomes requires the actin cytoskeleton.

We further studied the actin dependence of endocytic sterol trafficking by analyzing sterol distributions in *deformed root hairs 1* (*der1*) mutants defective in the *ACTIN2* (*ACT2*) gene [33]. *der1* mutants represent partial loss-of-function *act2* alleles that display root epidermal polarity defects [33]. In *der1* alleles, sterol distribution and FM4-64 internalization appeared normal (data not shown). By contrast, all three *der1* alleles were hypersensitive to treatment with 10 μM BFA for 30 min. BFA induced formation of 2–4 large sterol-positive compartments in *der1* mutants (Figures 6H and 6J; data not shown for *der1-3*) that are clearly distinct from the higher number of small punctate structures in BFA-treated wild-type cells (Figures 6G and 6I). Similarly, BFA differentially affected FM4-64 internalization and distribution in wild-type (Figure 6K) and *der1* epidermal cells (Figure 6L). Consistent with *der1* mutant phenotypes in epidermal differentiation [33], differences in sterol and FM4-64 distribution were observed in elongating and differentiated *der1* epidermal cells (Figures 6G–6L). The hypersensitivity of *der1* mutants to BFA-induced sterol and FM4-64 accumulation suggests that ACTIN2 is required for normal sterol distribution and early endocytic trafficking. The defects observed in *der1* closely resemble the effects of actin inhibitors on sterol redistribution from endosome agglomerations. These findings further support an actin requirement during redistribution events in early endocytic sterol trafficking.

Sterols and PIN2 Share a Common Endocytic Pathway

The cytoskeletal and vesicle transport requirements for early endocytic sterol trafficking resembled those described for PIN1 recycling in vascular cells [17]. However, the PM localization of another presumptive auxin transporter, the auxin influx carrier AUX1, can be modified by BFA treatment [34]. To address whether endocytic sterol trafficking is regulated by mechanisms similar to those governing the transport of PIN or AUX proteins, we examined sterol distributions in double labeling experiments with antibodies against epidermally expressed PIN2 [20] and hemagglutinin (HA) epitope-tagged AUX1 protein [35]. Sterols colabeled with PIN2 and HA-AUX1 at the PM of untreated epidermal cells

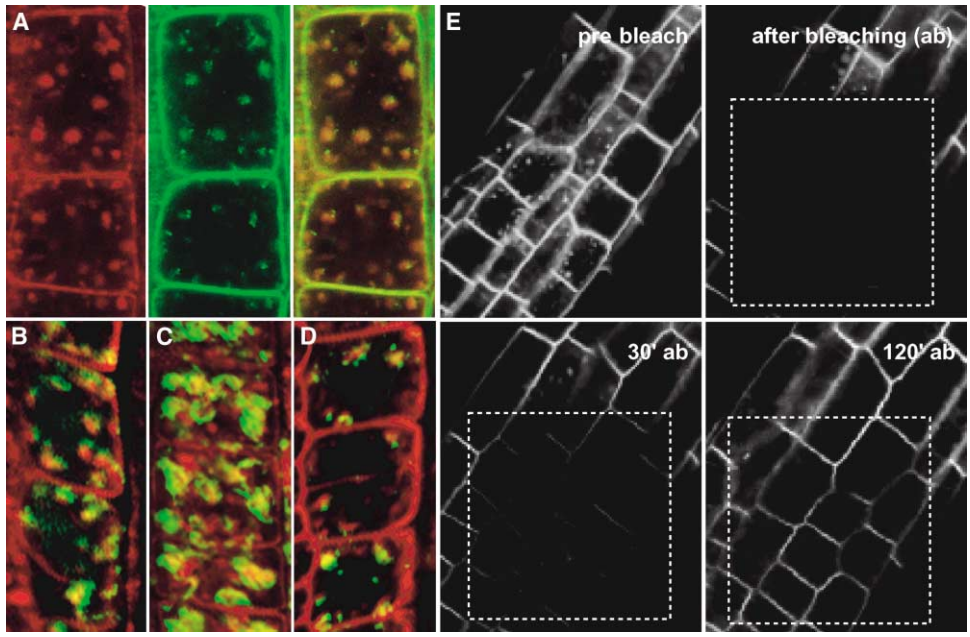

Figure 5. Actin-Dependent Endocytic Sterol Trafficking

(A–D) Filipin-sterol (red) costaining with GFP or YFP fusions (green) in cells fixed after 1 hr of incubation with 50 μM cytD. (A) Filipin-sterol and EGFP-LTI6a fluorescence. Right panel, merged channels. (B–D) Merged channels of filipin-sterol fluorescence colabeled with (B) ARA6-GFP, (C) NAG-EGFP, and (D) *N*-ST-YFP.

(E) FRAP analysis of EGFP-LTI6a fluorescence bleached after 1 hr of incubation with 50 μM cytD. FRAP was observed under continuous 50 μM cytD incubation at the indicated time points. The frames indicate areas of photobleaching.

(Figure 7). PIN2 and HA-AUX1 displayed their expected PM localizations toward the apical end or with a preferential apical-basal orientation, respectively (Figure 7) [20, 35]. Upon short-term BFA treatment, sterols colabeled with PIN2 in endosomal vesicle agglomerations, while PIN2 only partially maintained its apical localization at the PM (Figure 7). Under the same conditions, HA-AUX1 localization remained unaffected (data not shown). Extending the application period to 3 hr at 100 μM BFA caused almost complete loss of apical PIN2 from the PM and strong colabeling with sterols in BFA compartments (Figure 7). Under the same conditions, HA-AUX1 localization appeared more diffuse and depolarized when compared to untreated epidermal cells, but no distinct colocalization with sterols was observed in BFA-induced structures (Figure 7). Our findings demonstrate that BFA affects polar membrane localization of diverse PM proteins with different efficiency and specificity. They suggest that early endocytic sterol trafficking and polar PIN protein recycling follow a common BFA-sensitive endocytic pathway.

Discussion

We investigated early endocytic sterol trafficking in *Arabidopsis* by introducing filipin for fluorescent sterol visualization. Presently, filipin-based methods provide the only tools for in situ sterol localization in plants. Detection of 3-β-hydroxysterols allows analyses of bulk sterol distribution but does not discriminate between individual plant sterols. Nevertheless, biochemical studies revealed that relative compositions of individual sterols hardly differ between subcellular membrane fractions [23]. Consistent with this study, we detected high levels of plant sterols at the PM and partial colabeling with a marker that localizes to Golgi stacks and *trans*-Golgi cisternae. Restricted sterol accumulation along an organelle may reflect localization to certain substructures, as reported for the human Golgi, where *trans*-Golgi cisternae and vesicles are highly enriched in cholesterol [6].

Notably, filipin-based detection enabled us to observe sterol localization to early endosomes and to report on BFA-sensitive sterol endocytosis. Hitherto, BFA was solely thought to affect biosynthetic sterol trafficking at the plant Golgi [23], but, intriguingly, we found BFA-induced sterol accumulation in early endosomal aggregates that could be distinguished from Golgi stacks. Ultrastructural observations revealed the presence of only some *trans*-Golgi-derived material in such aggregations. Thus, upon short-term BFA treatment, only a subfraction of vesicles in these accumulations appears to derive from the Golgi. These findings are consistent with the observation that the *trans*-Golgi marker ST-myc localizes to BFA compartments after longer-term treatment at higher concentrations [32]. The rapid occurrence of PM-derived sterols and proteins in vesicle agglomerations that contain early endosomal markers demonstrates that sterol-enriched early endosomes provide a target for BFA interference in plants.

Interestingly, BFA caused fusion of early endosomes and the *trans*-Golgi-network (TGN) in animal cells, but, in contrast to our findings, this fusion network was dependent on intact microtubules [36, 37]. In *Arabidopsis*,

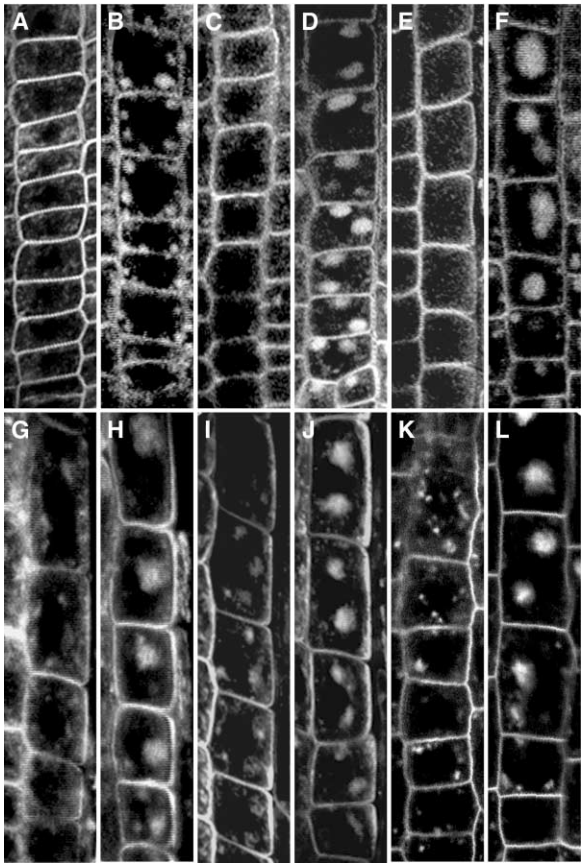

Figure 6. Actin-Dependent Sterol Redistribution from BFA Compartments

(A–J) Filipin-sterol fluorescence. (A) DMSO control. (B) 2.5 hr of incubation with 50 μM cytD. (C) 2.5 hr of incubation with 50 μM cytD and 2.5 hr of incubation with inhibitor-free medium. (D) 2.5 hr of incubation with 50 μM BFA. (E) 2.5 hr or incubation with 50 μM BFA and 2.5 hr of incubation with inhibitor-free medium. (F) 2.5 hr of incubation with 50 μM BFA, followed by wash out and 2.5 hr of incubation in 50 μM cytD. (G–J) Filipin-sterol fluorescence after 30 min of incubation with 10 μM BFA in (G and I) C24 wild-type, (H) *der1-1*, and (J) *der1-2*.

(K and L) FM4-64 internalization 30 min after labeling and incubation with 10 μM BFA in (K) C24 wild-type and (L) *der1-1*.

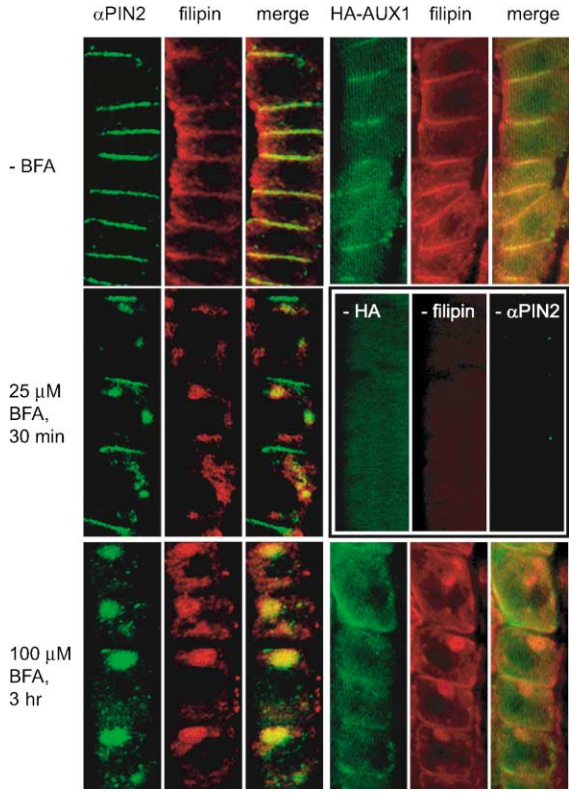

Figure 7. Early Endocytic Sterol and PIN2 Trafficking Share a Common Pathway

Double labeling for filipin-sterol fluorescence (red) with AtPIN2 or HA-tagged AUX1 (HA-AUX1) (green) detected by immunofluorescence localization. Upper row, without BFA. Middle row, left panels, 30 min of incubation with 25 μM BFA (PIN2 only). Middle row, right panels, Col controls without HA-AUX1 (−HA), without filipin (−filipin), or incubated without anti-AtPIN2 serum (−αPIN2). Bottom row, 3 hr of incubation with 100 μM BFA. Left panels, PIN2. Right panels, HA-AUX1.

sterol accumulation in BFA-induced endosomal aggregates was modified by actin-depolymerizing drugs and in *actin2* mutants. Sterol redistribution from endosomal aggregates proved actin dependent, and interference with the actin cytoskeleton induced colocalization of sterol-containing endosomes with the Golgi. These findings may reflect fundamental differences in cytoskeletal requirements for endocytic trafficking in plants and animals. Consistent with plant-specific modifications of early endocytic sterol trafficking, localization of ARA6-GFP proved actin dependent, while, in animal cells, Rab5 function is closely associated with tubulin-dependent transport [11]. The view that early endocytic transport in plants involves actin- rather than tubulin-based trafficking is supported by actin-dependent pectin endocytosis in maize [19] and PIN1 recycling in *Arabidopsis* roots [17].

It remains open via which organelle(s) sterols redistribute from early endosomes. The close association of BFA-induced, sterol-enriched endosome aggregations with *trans*-Golgi-derived material and the coaccumulation of sterols, endocytic, and Golgi markers upon cytD treatment may indicate that sterols could at least in part traffic between early endosomes and the Golgi (Figure 8). In animal cells, BFA partially inhibits transferrin receptor redistribution to the PM from the recycling endosome [38], a cholesterol-enriched compartment [7–9]. To our knowledge, BFA effects on sterol redistribution from early endosomes have not been reported in animal cells. Whether *Arabidopsis* sterols recycle directly from early endosomes or whether this involves equivalents to animal recycling endosomes remains another open question. So far, markers for plant recycling compartments are lacking, but sequences homologous to Rab proteins that regulate transport at animal recycling endosomes are present in the *Arabidopsis* genome [10]. In animal cells, recycling compartments and multivesicular bodies contain most of the cholesterol detected in the endocytic pathway [9]. Our ultrastructural analyses neither revealed a partially coated reticulum nor multivesicular bodies in sterol-enriched BFA compartments. In other

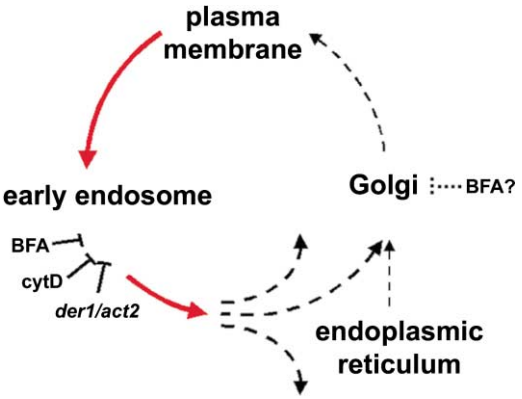

Figure 8. Model for Early Endocytic Sterol Trafficking in the *Arabidopsis* Root Epidermis

Early endocytic sterol trafficking requires the actin cytoskeleton (red arrows, actin-dependent trafficking). BFA targets sterol-enriched early endosomes, and sterol redistribution requires actin function. The redistribution pathways remain unknown (black dotted arrows). BFA inhibits biosynthetic sterol transport in other plants (black dotted arrows) [23], but it remains open whether similar mechanisms exist in *Arabidopsis* (question mark).

plant species, these structures have been interpreted as organelles analogous to animal recycling compartments and multivesicular bodies [15, 16]. Thus, the ultrastructural basis and further molecular composition of organelles involved in plant sterol endocytosis remains to be determined.

Despite lacking detailed knowledge on the endocytic pathway in *Arabidopsis*, the BFA-induced colabeling of sterols and PIN2 suggests that similar mechanisms regulate sterol endocytosis and PIN protein recycling. This interpretation is supported by recent findings of Geldner et al. [39]. They demonstrate that the *Arabidopsis* GNOM protein, a BFA-sensitive guanine-nucleotide exchange factor on ARF-type G proteins, mediates BFA-induced PIN1 accumulation in structures similar to the sterol-enriched early endosome agglomerations reported here. Additionally, GNOM-myc coaccumulates with PIN1 in BFA compartments, and GNOM-GFP colocalizes with FM4-64 early upon its internalization [39]. The localization of a BFA-sensitive ARF-GEF to early endosomal compartments in plants supports our view that early endocytic sterol trafficking provides a target for rapid BFA interference. However, it remains to be determined whether trafficking of sterol-enriched early endosomes is regulated by GNOM and/or whether other BFA-sensitive ARF-GEFs contribute to endocytic sterol transport in epidermal cells. The latter seems likely, since *gnom* mutations that render PIN1 trafficking fully insensitive to BFA confer only weak resistance on PIN2 transport [39], and we observed strong colocalization of sterols and PIN2 upon BFA treatment.

In contrast to similar effects on sterol and PIN2 trafficking, BFA exerted strikingly different action on epidermal AUX1 localization. These observations raise the question of whether sterols are involved in endocytic polar trafficking of specific PM components such as PIN family proteins. Consistent with a requirement of balanced sterol levels for polar PIN protein localization, we recently reported that PIN1 positioning is disturbed in the sterol biosynthesis mutant *orc* defective in *C-24 STEROL METHYLTRANSFERASE 1* (*SMT1*) [40]. Intriguingly, mutations in *erg6*, the budding yeast homolog of *SMT1* [40–42], affect polar positioning of protein and lipid raft components in the mating projection [43]. Thus, it will be interesting to determine whether polarity defects observed in the *smt1*^{orc} mutant are caused by changes in raft microdomain composition at the PM or by sterol-dependent polar sorting defects. The present study should open the door to further address functional roles of endocytic and biosynthetic sterol trafficking during the establishment of plant cell polarity.

Experimental Procedures

Plant Material and Growth Conditions

Seeds homozygous for *der1-1*, *der1-2*, or *der1-3* mutations [33] and from homozygous *aux1-22* plants expressing N-terminally HA-tagged AUX1 under its own promoter [35] were kindly provided by C. Ringli (Zürich, Switzerland) and M.J. Bennett (Nottingham, UK), respectively. Seeds from lines segregating *EGFP-Lti6a*, *EGFP-Lti6b*, and *EGFP-Q4* [28] were obtained from the Nottingham *Arabidopsis* stock center (UK) (stock numbers N84758, N84726, and N84728). mGFP5-ER was kindly made available by J. Haseloff (Cambridge, UK) (http://www.plantsci.cam.ac.uk/Haseloff/GFP/mgfpseq.html; [25]). Experiments included wild-type controls employing nontransformed Columbia (Col) or C24 ecotypes. Seeds were sterilized, imbibed for 3 days, and germinated on vertically oriented plates containing ½ MS agar, 1% sucrose (pH 5.8) as described previously [34]. Experiments were carried out on 5-day-old seedlings.

Inhibitor Treatments

For inhibitor treatments, per one well of a 24-well cell culture plate, 10–15 seedlings were incubated in 1 ml liquid medium (LM: ½ MS, 1% sucrose [pH 5.8]) containing the respective inhibitor or corresponding amounts of solvent. For recovery experiments, three 5-min LM washes were performed, and incubations continued under the conditions indicated. Incubations were stopped by fixation (see below). BFA was added from a 50 mM stock in dimethylsulfoxide (DMSO), cytD was added from a 25 mM stock in DMSO, and cycloheximide was added from a 50 mM stock in water. Inhibitors were purchased from Sigma. The data presented were reproduced in 3–10 independent experiments.

Generation of Plants Expressing GFP and YFP Fusion Proteins

The coding sequence for ARA6-GFP under control of the Cauliflower mosaic virus 35S promoter and nopaline synthase terminator [21] was excised with HindIII and EcoRI and was inserted into the corresponding sites of pBI121 (Clontech). The resulting vector was introduced into *Agrobacterium tumefaciens* strain C58C1. *N*-acetylglucosaminyl transferase I fused to fluorescent proteins has previously been employed as a Golgi marker [29]. The sequence for the transmembrane-stem regions of *Arabidopsis N*-acetylglucosaminyl transferase I (NAG; GenBank accession number AJ243198; [29]) was amplified from root cDNA employing primers *NAG-F*-BglII, 5′-GGGAGA TCTATGGCGAGGATCTCGTGTGACTTGA-3′, and *NAG-R*-XbaI, 5′-GGGTCTAGAAAGTTCTTCGTCCTGGCG-GTTCTTCA-3′. The product was subcloned into pBluescript II SK(-) (Stratagene) and was sequenced. The resulting BglII/XbaI fragment was inserted in frame to the N terminus of EGFP (Clontech) engineered in pGreenII0229 between the Cauliflower mosaic virus 35S promoter and nopaline synthase terminator [44] (http://www.pgreen.ac.uk). An *N*-ST-GFP construct [27] was modified by exchanging the GFP sequence for YFP. The resulting vector was transformed into *A. tumefaciens* C58 (GV3101) and was kindly made available by M. Batoko and I.A. Moore (Oxford, UK). Constructs were introduced into *Arabidopsis* plants ecotype Col by *Agrobacterium*-mediated transformation [45]. Analyses were performed on segregating T2 lines or homozygote T3 lines from several independent transformants. No obvious differ-

ences in colabeling between filipin and GFP fusion proteins expressed in the heterozygote or homozygote situation were observed.

Detection of Filipin-Sterol Fluorescence in *Arabidopsis* Roots

A microwave-accelerated staining and fixation protocol for plant F-actin [46] was modified for detection of filipin-sterol fluorescence. Seedlings were transferred to 4% paraformaldehyde (PFA), 0.1–0.2 mg/ml filipin III (Sigma) (from a 10–20 mg/ml stock in DMSO) in microtubule-stabilizing buffer (MTSB: 50 mM Pipes, 5 mM EGTA, 5 mM $MgSO_4$ [pH 7.0]) [47] in a final volume of 500 μl. Samples were placed into an M959 conventional microwave oven (Samsung) and were pulsed six times for 30 s at 90 W; there was a 1-min pause in between intervals. Under these conditions, the sample temperature did not exceed 35°C–40°C. Sample staining/fixation was extended to 1 hr at room temperature. Specimens were washed three times in demineralized water (demin H_2O), and roots were mounted in Citifluor AF1 antifade reagent (Citifluor) for observation by confocal laser scanning microscopy (CLSM).

Immunocytochemistry of Antibody-Filipin Double Labels

Immunofluorescence localization [20, 35, 47] was modified for concomitant antibody staining and sterol visualization by replacing the detergent with filipin. For details on filipin-sterol/antibody immunocytochemistry, see the Supplemental Data.

FRAP Analysis of GFP Fusion Proteins

FRAP analysis of GFP fusions was performed by employing a Leica TCS SP2 system attached to a Leica DM IRB inverted confocal microscope (Leica) using the 488 nm line of an Ar/Kr laser (see the Supplemental Data for details).

Filipin-Sterol, FM4-64, and GFP/YFP Fluorescence Analyses in Live Roots

Arabidopsis seedlings expressing GFP or YFP fusion proteins and nontransformed seedlings were incubated with 50 μM FM4-64 (Molecular Probes) and/or 20 μg/ml filipin III in LM for 10 min on ice, washed twice with medium, incubated for indicated periods at room temperature, and observed by CLSM and/or two-photon LSM.

Two-Photon/Confocal Laser Scanning and Electron Microscopy

See the Supplemental Data for methodological details on CLSM, two-photon LSM, and electron microscopy.

Supplemental Data

Supplemental Data including detailed Experimental Procedures, additional references, and two figures accompanies the on-line version of this article at http://www.current-biology.com/cgi/content/full/13/16/1378/DC1/.

Acknowledgments

We gratefully acknowledge H. Batoko, M.J. Bennett, J. Haseloff, I.A. Moore, K. Palme, C. Ringli, C.R. Somerville, and R. Swarup for making available materials used in this study and the *Arabidopsis* Stock Centres for providing seed stocks. We thank M. Aida, R. Heidstra, D. Welch, and V. Willemsen for critical reading of the manuscript. This work was supported by a Marie Curie postdoctoral fellowship (HPMF-CT-2000-00969) of the European Community Framework Programme V to M.G. and a PIONIER award of the Dutch Organization for Sciences (NWO) to B.S.

Received: February 21, 2003
Revised: May 23, 2003
Accepted: June 26, 2003
Published: August 19, 2003

References

1. Keller, P., and Simons, K. (1998). Cholesterol is required for surface transport of influenza virus hemagglutinin. J. Cell Biol. *140*, 1357–1367.
2. Michaux, G., Gansmuller, A., Hindelang, C., and Labouesse, M. (2000). CHE-14, a protein with a sterol-sensing domain, is required for apical sorting in *C. elegans* ectodermal epithelial cells. Curr. Biol. *10*, 1098–1107.
3. Ingham, P.W. (2001). Hedgehog signaling: a tale of two lipids. Science *294*, 1879–1881.
4. Ioannou, Y.A. (2001). Multidrug permeases and subcellular cholesterol transport. Nat. Rev. Mol. Cell Biol. *2*, 657–668.
5. Mellman, I. (1996). Endocytosis and molecular sorting. Annu. Rev. Cell Dev. Biol. *12*, 575–625.
6. Orci, L., Montesano, R., Meda, P., Malaisse-Lagae, F., Brown, D., Perrelet, A., and Vassalli, P. (1981). Heterogeneous distribution of filipin-cholesterol complexes across the cisternae of the Golgi apparatus. Proc. Natl. Acad. Sci. USA *78*, 293–297.
7. Gagescu, R., Demaurex, N., Parton, R.G., Hunziker, W., Huber, L.A., and Gruenberg, J. (2000). The recycling endosome of Madin-Darby canine kidney cells is a mildly acidic compartment rich in raft components. Mol. Biol. Cell *11*, 2775–2791.
8. Hölttä-Vuori, M., Tanhuanpää, K., Möbius, W., Somerharju, P., and Ikonen, E. (2002). Modulation of cellular cholesterol transport and homeostasis by Rab11. Mol. Biol. Cell *13*, 3107–3122.
9. Möbius, W., van Donselaar, E., Ohno-Iwashita, Y., Shimada, Y., Heijnen, H.F.G., Slot, J.W., and Geuze, H.J. (2003). Recycling compartments and the internal vesicles of multivesicular bodies harbor most of the cholesterol found in the endocytic pathway. Traffic *4*, 221–231.
10. Rutherford, S., and Moore, I. (2002). The *Arabidopsis* Rab GTPase family: another enigma variation. Curr. Opin. Plant Biol. *5*, 518–528.
11. Nielsen, E., Severin, F., Backer, J.M., Hyman, A.A., and Zerial, M. (1999). Rab5 regulates motility of early endosomes on microtubules. Nat. Cell Biol. *1*, 376–382.
12. Matteoni, R., and Kreis, T.E. (1987). Translocation and clustering of endosomes and lysosomes depends on microtubules. J. Cell Biol. *105*, 1253–1265.
13. Heino, S., Lusa, S., Somerharju, P., Ehnholm, C., Olkkonen, V.M., and Ikonen, E. (2000). Dissecting the role of the Golgi complex and lipid rafts in biosynthetic transport of cholesterol to the cell surface. Proc. Natl. Acad. Sci. USA *97*, 8375–8380.
14. Neufeld, E.B., Cooney, A.M., Pitha, J., Dawidowicz, E.A., Dwyer, N.K., Pentchev, P.G., and Blanchette-Mackie, E.J. (1996). Intracellular trafficking of cholesterol monitored with a cyclodextrin. J. Biol. Chem. *271*, 21604–21613.
15. Low, P.S., and Chandra, S. (1994). Endocytosis in plants. Annu. Rev. Plant Physiol. Plant Mol. Biol. *45*, 609–631.
16. Holstein, S.E.H. (2002). Clathrin and plant endocytosis. Traffic *3*, 614–620.
17. Geldner, N., Friml, J., Stierhof, Y.-D., Jürgens, G., and Palme, K. (2001). Auxin transport inhibitors block PIN1 cycling and vesicle trafficking. Nature *413*, 425–428.
18. Shah, K., Russinova, E., Gadella, T.W., Jr., Willemse, J., and de Vries, S.C. (2002). The *Arabidopsis* kinase-associated protein phosphatase controls internalization of the somatic embryogenesis receptor kinase 1. Genes Dev. *16*, 1707–1720.
19. Baluska, F., Hlavacka, A., Samaj, J., Palme, K., Robinson, D.G., Matoh, T., McCurdy, D.W., Menzel, D., and Volkmann, D. (2002). F-actin-dependent endocytosis of cell wall pectins in meristematic root cells. Insights from brefeldin A-induced compartments. Plant Physiol. *130*, 422–431.
20. Müller, A., Guan, C., Gälweiler, L., Tänzler, P., Huijser, P., Marchant, A., Parry, G., Bennett, M., Wisman, E., and Palme, K. (1998). AtPIN2 defines a locus of *Arabidopsis* for root gravitropism control. EMBO J. *17*, 6903–6911.
21. Ueda, T., Yamaguchi, M., Uchimiya, H., and Nakano, A. (2001). Ara6, a plant-unique novel type Rab GTPase, functions in the endocytic pathway of *Arabidopsis thaliana*. EMBO J. *20*, 4730–4741.
22. Benveniste, P. (1986). Sterol biosynthesis. Annu. Rev. Plant Physiol. *37*, 275–308.

23. Moreau, P., Hartmann, M.-A., Perret, A.M., Sturbois-Balcerzak, B., and Cassagne, C. (1998). Transport of sterols to the plasma membrane of leek seedlings. Plant Physiol. *117*, 931–937.
24. Nebenführ, A., Ritzenthaler, C., and Robinson, D.G. (2002). Brefeldin A: deciphering an enigmatic inhibitor of secretion. Plant Physiol. *130*, 1102–1108.
25. Haseloff, J., Siemering, K.R., Prasher, D.C., and Hodge, S. (1997). Removal of a cryptic intron and subcellular localisation of green fluorescent protein are required to mark transgenic *Arabidopsis* plants brightly. Proc. Natl. Acad. Sci. USA *94*, 2122–2127.
26. Boevink, P., Oparka, K., Santa Cruz, S., Martin, B., Betteridge, A., and Hawes, C. (1998). Stacks on tracks: the plant Golgi apparatus traffics on an actin/ER network. Plant J. *15*, 441–447.
27. Batoko, H., Zheng, H.Q., Hawes, C., and Moore, I.A. (2000). rab1 GTPase is required for transport between the endoplasmic reticulum and Golgi apparatus and for normal Golgi movement in plants. Plant Cell *12*, 2201–2218.
28. Cutler, S.R., Ehrhardt, D.W., Griffitts, J.S., and Somerville, C.R. (2000). Random GFP::cDNA fusions enable visualization of subcellular structures in cells of *Arabidopsis* at a high frequency. Proc. Natl. Acad. Sci. USA *97*, 3718–3723.
29. Dixit, R., and Cyr, R. (2002). Golgi secretion is not required for marking the preprophase band site in cultured tobacco cells. Plant J. *29*, 99–108.
30. Capel, J., Jarillo, J.A., Salinas, J., and Martinez-Zapater, J. (1997). Two homologous low-temperature-inducible genes from *Arabidopsis* encode highly hydrophobic proteins. Plant Physiol. *115*, 569–576.
31. Navarre, C., and Goffeau, A. (2000). Membrane hyperpolarization and salt sensitivity induced by deletion of PMP3, a highly conserved small protein of yeast plasma membrane. EMBO J. *19*, 2515–2524.
32. Wee, E.G., Sherrier, D.J., Prime, T.A., and Dupree, P. (1998). Targeting of active sialyltransferase to the plant Golgi apparatus. Plant Cell *10*, 1759–1768.
33. Ringli, C., Baumberger, N., Diet, A., Frey, B., and Keller, B. (2002). ACTIN2 is essential for bulge site selection and tip growth during root hair development of *Arabidopsis*. Plant Physiol. *129*, 1464–1472.
34. Grebe, M., Friml, J., Swarup, R., Ljung, K., Sandberg, G., Terlou, M., Palme, K., Bennett, M.J., and Scheres, B. (2002). Cell polarity signaling in *Arabidopsis* involves a BFA-sensitive auxin influx pathway. Curr. Biol. *12*, 329–334.
35. Swarup, R., Friml, J., Marchant, A., Ljung, K., Sandberg, G., Palme, K., and Bennett, M. (2001). Localization of the auxin permease AUX1 suggests two functionally distinct hormone transport pathways operate in the *Arabidopsis* root apex. Genes Dev. *15*, 2648–2653.
36. Wood, S.A., Park, J.E., and Brown, W.J. (1991). Brefeldin A causes a microtubule mediated fusion of the trans-Golgi network and early endosomes. Cell *67*, 591–600.
37. Lippincott-Schwartz, J., Yuan, L., Tipper, C., Amherdt, M., Orci, L., and Klausner, R.D. (1991). Brefeldin A's effect on endosomes, lysosomes, and the TGN suggests a general mechanism for regulating organelle structure and membrane traffic. Cell *67*, 601–616.
38. Van Dam, E.M., Ten Broeke, T., Jansen, K., Spijkers, P., and Stoorvogel, W. (2002). Endocytosed transferrin receptors recycle via distinct dynamin and phosphatidylinositol 3-kinase-dependent pathways. J. Biol. Chem. *277*, 48876–48883.
39. Geldner, N., Anders, N., Wolters, H., Keicher, J., Kornberger, W., Muller, P., Delbarre, A., Ueda, T., Nakano, A., and Jürgens, G. (2003). The *Arabidopsis* GNOM ARF-GEF mediates endosomal recycling, auxin transport, and auxin-dependent plant growth. Cell *112*, 219–230.
40. Willemsen, V., Friml, J., Grebe, M., van den Toorn, A., Palme, K., and Scheres, B. (2003). Cell polarity and PIN protein positioning in *Arabidopsis* require STEROL METHYLTRANSFFERASE1 function. Plant Cell *15*, 612–625.
41. Diener, A.C., Li, H., Zhou, W., Whoriskey, W.J., Nes, W.D., and Fink, G.R. (2000). Sterol methyltransferase 1 controls the level of cholesterol in plants. Plant Cell *12*, 853–870.
42. Schrick, K., Mayer, U., Martin, G., Bellini, C., Kuhnt, C., Schmidt, J., and Jürgens, G. (2002). Interactions between sterol biosynthesis genes in embryonic development of *Arabidopsis*. Plant J. *31*, 61–73.
43. Bagnat, M., and Simons, K. (2002). Cell surface polarization during yeast mating. Proc. Natl. Acad. Sci. USA *99*, 14183–14188.
44. Hellens, R.P., Edwards, E.A., Leyland, N.R., Bean, S., and Mullineaux, P.M. (2000). PGreen: a versatile and flexible binary Ti vector for Agrobacterium-mediated plant transformation. Plant Mol. Biol. *42*, 819–832.
45. Clough, S.J., and Bent, A.F. (1998). Floral dip: a simplified method for Agrobacterium-mediated transformation of *Arabidopsis thaliana*. Plant J. *16*, 735–743.
46. Sawitzky, H., Willingale-Theune, J., and Menzel, D. (1996). Improved visualization of F-actin in the green alga Acetabularia by microwave-accelerated fixation and simultaneous FITC-Phalloidin staining. Histochem. J. *28*, 353–360.
47. Lauber, M.H., Waizenegger, I., Steinmann, T., Schwarz, H., Mayer, U., Hwang, I., Lukowitz, W., and Jürgens, G. (1997). The *Arabidopsis* KNOLLE protein is a cytokinesis-specific syntaxin. J. Cell Biol. *139*, 1485–1493.